

# LONG-RUN AVAILABILITY OF A PRIORITY SYSTEM: A NUMERICAL APPROACH

EDMOND J. VANDERPERRE AND STANISLAV S. MAKHANOV

*Received 29 June 2004*

We consider a two-unit cold standby system attended by two repairmen and subjected to a priority rule. In order to describe the random behavior of the twin system, we employ a stochastic process endowed with state probability functions satisfying coupled Hokstad-type differential equations. An explicit evaluation of the exact solution is in general quite intricate. Therefore, we propose a numerical solution of the equations. Finally, particular but important repair time distributions are involved to analyze the long-run availability of the **T**-system. Numerical results are illustrated by adequate computer-plotted graphs.

## 1. Introduction

Standby provides a powerful tool to enhance the reliability, availability, quality, and safety of operational plants, see, for example, [3, 7, 14]. However, in practice, standby systems are often subjected to an appropriate priority rule. For instance, the *external* power supply station of a technical plant has usually overall priority in operation with regard to an *internal* (local) power generator kept in cold or warm standby [3]. The local generator is only deployed if the external power station is down.

Cold or warm standby systems subjected to a priority rule and attended by a repair facility have received considerable attention in the current literature, see, for example, [1, 2, 4, 5, 8, 9, 10, 11, 12, 13, 16, 17, 18, 19, 20, 21].

As a variant, we consider a twin system composed of a priority unit (the **p**-unit) and a nonpriority unit (the **n**-unit) kept in *cold* standby. The **p**-unit has *overall* (break-in) priority in operation with regard to the **n**-unit, that is, the **n**-unit is only used when the **p**-unit is down. In order to avoid undesirable delays in repairing failed units, we suppose that the entire system (henceforth called the **T**-system) is attended by *two* different repairmen. The **T**-system satisfies the usual conditions, that is, independent identically distributed random variables, instantaneous and perfect switch [3], and perfect repair [6]. Each repairman has his own particular task. Repairman  $\mathcal{N}$  is skilled in repairing the **n**-unit, whereas repairman  $\mathcal{P}$  is an expert in repairing the **p**-unit. Both repairmen are jointly busy, if and only if, both units (**p**-unit and **n**-unit) are down. In any other case, at least one repairman is idle.

In order to describe the *random* behavior of the **T**-system, we employ a stochastic process endowed with transition probability functions satisfying steady-state Hokstad-type differential equations. Unfortunately, the *exact* solution procedure is quite intricate (see, [21, page 359] and Remark 4.1). Therefore, we propose a *numerical* solution of the equations.

Finally, current repair time distributions (such as the Weibull-Gnedenko distribution) are involved to compute the long-run availability of the **T**-system. The results are illustrated by adequate computer-plotted graphs.

## 2. Formulation

Consider a **T**-system satisfying the usual conditions. The **p**-unit has a constant failure rate [15]  $\lambda > 0$  and a general repair time distribution  $R(\cdot), R(0) = 0$ , with mean  $\rho$ . The *operative* **n**-unit has a constant failure rate  $\lambda_s > 0$ , but a *zero* failure rate in standby (the so-called cold standby state) and a general repair time distribution  $R_S(\cdot), R_S(0) = 0$ , with mean  $\rho_s$ . In order to describe the random behavior of the **T**-system, we introduce a stochastic process  $\{N_t, t \geq 0\}$  with arbitrary discrete state space  $\{A, B, C, D\} \subset [0, \infty)$ , characterized by the following mutually exclusive events:

- (i)  $\{N_t = A\}$ : “the **p**-unit is operative and the **n**-unit is in cold standby at time  $t$ ,”
- (ii)  $\{N_t = B\}$ : “the **n**-unit is operative and the **p**-unit is under repair at time  $t$ ,”
- (iii)  $\{N_t = C\}$ : “the **p**-unit is operative and the **n**-unit is under repair at time  $t$ ,”
- (iv)  $\{N_t = D\}$ : “both units are simultaneously down at time  $t$ .”

State  $D$  is called the system-down state.

Figures 2.1, 2.2, 2.3, and 2.4 display a functional block diagram of the **T**-system operating in states  $A, B, C$ , and  $D$ .

Observe that the process  $\{N_t, t \geq 0\}$  is non-Markovian. A Markov characterization of the process is piecewise and conditionally defined by:

- (i)  $\{N_t\}$ , if  $N_t = A$  (i.e., if the event  $\{N_t = A\}$  occurs),
- (ii)  $\{(N_t, X_t)\}$ , if  $N_t = B$ , where  $X_t$  denotes the *remaining* repair time of the **p**-unit under progressive repair at time  $t$ ,
- (iii)  $\{(N_t, Y_t)\}$ , if  $N_t = C$ , where  $Y_t$  denotes the *remaining* repair time of the **n**-unit under progressive repair at time  $t$ ,
- (iv)  $\{(N_t, X_t, Y_t)\}$ , if  $N_t = D$ .

The state space of the underlying piecewise linear (vector) Markov process is given by

$$A \cup \{(B, x); x \geq 0\} \cup \{(C, y); y \geq 0\} \cup \{(D, x, y); x \geq 0; y \geq 0\}. \quad (2.1)$$

Next, we consider the **T**-system in stationary state (the so-called *ergodic* state) with *invariant* measure  $\{p_K; K = A, B, C, D\}$ ,  $\sum_K p_K = 1$ , where

$$p_K := \lim_{t \rightarrow \infty} \mathbf{P}\{N_t = K | N_0 = A\}. \quad (2.2)$$

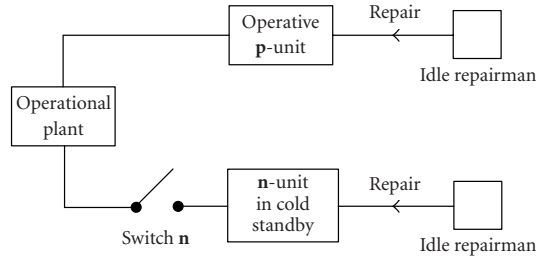


Figure 2.1. Functional block diagram of the T-system operating in state A.

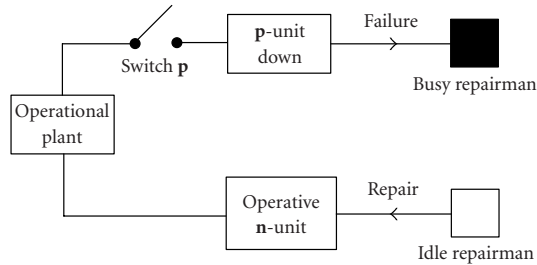


Figure 2.2. Functional block diagram of the T-system operating in state B.

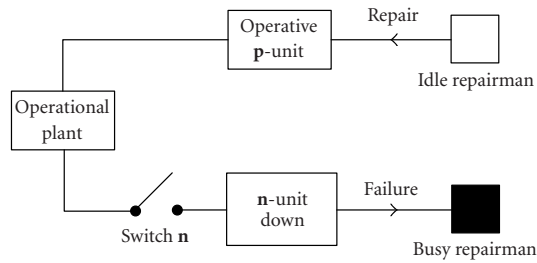


Figure 2.3. Functional block diagram of the T-system operating in state C.

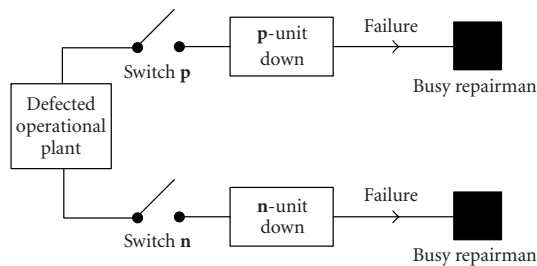


Figure 2.4. Functional block diagram of the T-system in state D.

It can be demonstrated that the invariant measure exists for arbitrary  $R$  and  $R_S$  with finite mean. However, in order to keep the analysis as simple as possible, we henceforth assume that  $R$  and  $R_S$  have *bounded* densities on  $[0, \infty)$ , denoted by  $r$  and  $r_s$ . Finally, we introduce the measures

$$\begin{aligned} p_B(x)dx &:= \lim_{t \rightarrow \infty} \mathbf{P}\{N_t = B, X_t \in (x, x + dx) | N_0 = A\}, \\ p_C(y)dy &:= \lim_{t \rightarrow \infty} \mathbf{P}\{N_t = C, Y_t \in (y, y + dy) | N_0 = A\}, \\ p_D(x, y)dx dy &:= \lim_{t \rightarrow \infty} \mathbf{P}\{N_t = D, X_t \in (x, x + dx), Y_t \in (y, y + dy) | N_0 = A\}. \end{aligned} \quad (2.3)$$

Note that, for instance,  $p_D = \int_0^\infty \int_0^\infty p_D(x, y)dx dy$ .

### 3. Long-run availability

We recall that the  $\mathbf{T}$ -system is only available (functioning) in states  $A$ ,  $B$ , and  $C$ . Therefore, the *long-run* availability of the operational plant, denoted by  $\mathcal{A}$ , is given by  $\mathcal{A} = 1 - p_D$ . Invoking the substitutions  $p_B(\cdot) = p_A \varphi_B(\cdot)$ ,  $p_C(\cdot) = p_A \varphi_C(\cdot)$ ,  $p_D(\cdot, \cdot) = p_A \varphi_D(\cdot, \cdot)$  and the law  $\sum_K p_K = 1$  entails that  $p_A = 1/(1 + \Phi_B + \Phi_C + \Phi_D)$ , where  $\Phi_B := \int_0^\infty \varphi_B(x)dx$ ,  $\Phi_C := \int_0^\infty \varphi_C(y)dy$  and  $\Phi_D := \int_0^\infty \int_0^\infty \varphi_D(x, y)dx dy$ . Hence,

$$\mathcal{A} = \frac{1 + \Phi_B + \Phi_C}{1 + \Phi_B + \Phi_C + \Phi_D}. \quad (3.1)$$

### 4. Differential equations

In order to determine the  $\varphi$ -functions, we first construct a system of coupled steady state-type differential equations based on a time-independent version of Hokstad's supplementary variable technique (see, e.g., [22, page 526] for further details). For  $x > 0$ ,  $y > 0$ , we obtain

$$\lambda = \varphi_B(0) + \varphi_C(0), \quad (4.1)$$

$$\left(\lambda_s - \frac{d}{dx}\right) \varphi_B(x) = \varphi_D(x, 0) + \lambda r(x), \quad (4.2)$$

$$\left(\lambda - \frac{d}{dy}\right) \varphi_C(y) = \varphi_D(0, y), \quad (4.3)$$

$$\left(-\frac{\partial}{\partial x} - \frac{\partial}{\partial y}\right) \varphi_D(x, y) = \lambda_s \varphi_B(x) r_s(y) + \lambda \varphi_C(y) r(x). \quad (4.4)$$

*Remark 4.1.* A particular but important family  $\mathcal{F}$  of current repair time distributions with nonrational characteristic functions, such as the Weibull-Gnedenko and Lognormal distributions, are fairly suitable to model repair times. Unfortunately, if both  $R$  and  $R_S$  belong to  $\mathcal{F}$ , an explicit evaluation of the *exact* solution of (4.1), (4.2), (4.3), and (4.4) in terms of *finite* linear combinations of known algebraic and/or transcendental functions is as good as excluded (see [21, page 361] for further details). Therefore, we propose a *numerical* solution of the equations.

### 5. Numerical scheme

In order to construct an appropriate numerical procedure, we first remark that the  $\varphi$ -functions are vanishing at infinity *irrespective* of the asymptotic behavior of the repair time density functions! Therefore, a numerical procedure to solve the equations in the region  $(0, \infty) \times (0, \infty)$  may be converted into a numerical solution procedure in the *truncated* region  $(0, L) \times (0, L)$ , for some  $L > 0$ , with prescribed boundary conditions  $\varphi_B(L) = \varphi_C(L) = \varphi_D(L, \cdot) = \varphi_D(\cdot, L) = 0$ . Let  $\varphi_{B,i} := \varphi_B(x_i)$ ,  $\varphi_{C,j} := \varphi_C(y_j)$ ,  $\varphi_{D,i,j} := \varphi_D(x_i, y_j)$ , where  $x_i := i\Delta$ ,  $y_j := j\Delta$ ,  $i = 0, \dots, N + 1$ ;  $j = 0, \dots, N + 1$ ;  $\Delta := L/N$ . We propose the following numerical scheme. Let  $k$  be the iteration number. Given  $\varphi_{D,i,N+1}^{k+1} = 0$ ,  $\varphi_{D,N+1,j}^{k+1} = 0$ ,  $\varphi_{B,N+1}^{k+1} = 0$ ,  $\varphi_{C,N+1}^{k+1} = 0$ , and the values of  $\varphi_{B,i}^k$  and  $\varphi_{C,j}^k$ , we compute  $\varphi_{D,i,j}^{k+1}$  by means of the two-point first-order approximation of (4.4), namely,

$$\varphi_{D,i,j}^{k+1} = \frac{1}{2}(\varphi_{D,i,j+1}^{k+1} + \varphi_{D,i+1,j}^{k+1}) + \frac{\Delta}{2}(\lambda_s \varphi_{B,i}^k r_{s,j} + \lambda \varphi_{C,j}^k r_i), \tag{5.1}$$

$i = N, N - 1, \dots, 0$  and  $j = N, N - 1, \dots, 0$ .

Next, we calculate  $\varphi_{B,i}^{k+1}$  and  $\varphi_{C,j}^{k+1}$  by means of the first-order approximations of (4.2) and (4.3) given by

$$\begin{aligned} \varphi_{B,i}^{k+1} &= \frac{1}{\gamma_B} \left( \frac{\varphi_{B,i+1}^{k+1}}{\Delta} + \varphi_{D,i,0}^{k+1} + \lambda r_i \right), \\ \varphi_{C,j}^{k+1} &= \frac{1}{\gamma_C} \left( \frac{\varphi_{C,j+1}^{k+1}}{\Delta} + \varphi_{D,0,j}^{k+1} \right), \end{aligned} \tag{5.2}$$

where  $\gamma_B := \lambda_s + 1/\Delta$  and  $\gamma_C := \lambda + 1/\Delta$ . Finally, in order to satisfy (4.1) we use the normalizing procedure

$$\begin{aligned} \varphi_{C,j}^{k+1, \text{new}} &= \lambda \frac{\varphi_{C,j}^{k+1}}{\varphi_{C,0}^{k+1} + \varphi_{B,0}^{k+1}}, \\ \varphi_{B,i}^{k+1, \text{new}} &= \lambda \frac{\varphi_{B,i}^{k+1}}{\varphi_{C,0}^{k+1} + \varphi_{B,0}^{k+1}}. \end{aligned} \tag{5.3}$$

*Remarks 5.1.* Let  $\varphi_\Delta$  denote a numerical solution obtained with the space-step  $\Delta$ . The relevant numerical error is then evaluated on a nested grid by  $\varepsilon := |\varphi_\Delta - \varphi_{\Delta/2}|$ . However, such an estimate is only accurate if  $L$  is large enough. Roughly speaking, if  $\max(r(x), r_s(x))$  at  $x = L$  is small, then (most likely) this particular  $L$  is appropriate. However, such a “brutal force” approach may require a large number of grid points and is therefore rarely applicable. We illustrate the phenomenon by comparing the exact and the numerical solution in the most simple case, that is, let  $R(x) = 1 - e^{-x}$ ,  $R_S(y) = 1 - e^{-y}$ . Then,  $\varphi_D(x, y) = l_D e^{-(x+y)}$ ,  $\varphi_C(y) = l_C e^{-y}$ ,  $\varphi_B(x) = l_B e^{-x}$ , where  $l_D := \lambda_s(\lambda + 1)\lambda/(\lambda_s + \lambda + 2)$ ,  $l_C := \lambda_s\lambda/(\lambda_s + \lambda + 2)$ ,  $l_B := \lambda(\lambda + 2)/(\lambda_s + \lambda + 2)$ .

Figure 5.1 shows the numerical error

$$\varepsilon_M := \max \{ |\varphi_D^{\text{exact}} - \varphi_D|, |\varphi_C^{\text{exact}} - \varphi_C|, |\varphi_B^{\text{exact}} - \varphi_B| \} \tag{5.4}$$

versus the grid size for various  $L$ .

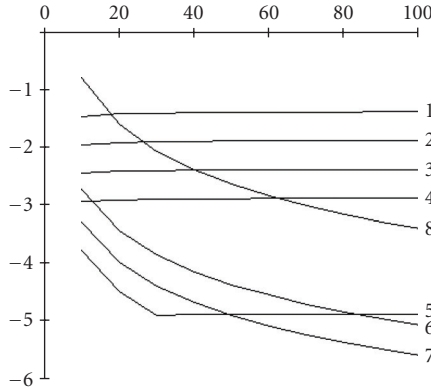


Figure 5.1. The horizontal axis denotes the logarithm of the numerical error, the vertical axis denotes the number of the grid points, (1)  $L = 0.4$ ; (2)  $L = 1.0$ ; (3)  $L = 1.5$ ; (4)  $L = 2$ ; (5)  $L = 4$ ; (6)  $L = 6$ ; (7)  $L = 10$ ; (8)  $L = 50$ .

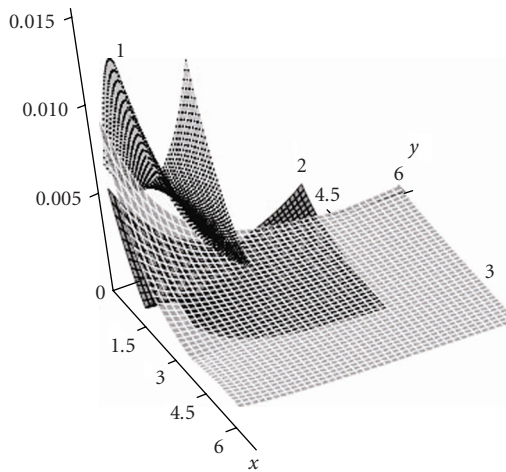


Figure 5.2. Spatial distribution of  $\varepsilon_D$ , (1)  $L = 1.5$ ; (2)  $L = 3$ ; (3)  $L = 6$ .

Observe that, if  $L$  is not large enough,  $\varepsilon_M$  does not decrease as  $\Delta$  decreases (see Figure 5.1). On the other hand, too large  $L$  (consequently, too large  $\Delta$ ) lead to large numerical errors. For instance, the error with  $L = 30$  is larger than  $2.5 \cdot 10^{-2}$  for any  $N \in [20, 100]$ , whereas the error with  $L = 4$  is less than  $2.5 \cdot 10^{-2}$ . There could be multiple options too. For instance, an error less than  $2.5 \cdot 10^{-2}$  is achieved either with  $L = 4$ ,  $N = 15$ , or  $L = 6$ ,  $N = 22$ , or  $L = 10$ ,  $N = 38$ .

Figure 5.2 shows a two-dimensional spatial distribution of the error  $\varepsilon_D := |\varphi_D^{\text{exact}} - \varphi_D|$  for various  $L$ . Clearly,  $\varepsilon_D$  could be increasing near the origin as  $L$  increases. However, the error decreases for large  $x$  and  $y$ .

**6. Trial-and-error procedure**

The complicated behavior of the numerical error requires an adaptive choice of  $\Delta$  and  $L$ . Therefore, we introduce the subordinate errors  $\varepsilon_1 := |\varphi_{\Delta,L} - \varphi_{\Delta,L/2}|$  and  $\varepsilon_2 := |\varphi_{\Delta,L} - \varphi_{\Delta/2,L}|$ , where  $\varepsilon_1$  characterizes the numerical error caused by truncation of the infinite region and  $\varepsilon_2$  the numerical error related to the first-order approximants. In order to find the optimal pair  $(L, \Delta)$ , we first specify the required accuracy  $\varepsilon$ . Next, we propose the following trial-and-error procedure: *we vary  $L$  until  $\varepsilon_1 < \varepsilon$  and then  $\Delta$  until  $\varepsilon_2 < \varepsilon$* . Finally, we introduce the following.

**7. Application. The Weibull-Gnedenko distribution**

We consider the particular but important case of Weibull-Gnedenko repair time distributions, that is, let  $R(x) = 1 - e^{-x^{\beta_1}}$ ,  $R_S(y) = 1 - e^{-y^{\beta_2}}$ . Obviously, the optimal pair  $(L, \Delta)$  depends on  $\lambda, \lambda_s, \beta_1$ , and  $\beta_2$ . We demonstrate the trial-and-error procedure applied to the particular case  $\lambda = 1, \lambda_s = 0.1, \beta_1 = 2, \beta_2 = 3$ . However, no restrictions are imposed on the analysis of  $\mathcal{A}$  for arbitrary values of  $\lambda, \lambda_s, \beta_1$  and  $\beta_2$ . Let  $\varepsilon = 10^{-3}$ .

First, we vary  $L$ , as shown in Table 7.1, until  $\varepsilon_1 < \varepsilon$ . Next, we vary  $\Delta$ , as shown in Table 7.2, until  $\varepsilon_2 < \varepsilon$ . A spatial distribution of  $\varepsilon_1$  and  $\varepsilon_2$  is depicted in Figures 7.1 and 7.2.

Table 7.1. The  $L$  trials.

| $L$ | $N$ | $\Delta$ | $\varepsilon_1$     |
|-----|-----|----------|---------------------|
| 3   | 40  | 3/40     | $1.9 \cdot 10^{-2}$ |
| 6   | 80  | 3/40     | $7.4 \cdot 10^{-4}$ |

Table 7.2. The  $\Delta$  trials.

| $L$ | $N$ | $\Delta$ | $\varepsilon_2$     |
|-----|-----|----------|---------------------|
| 6   | 80  | 3/40     | $6.8 \cdot 10^{-3}$ |
| 6   | 160 | 3/80     | $3.3 \cdot 10^{-3}$ |
| 6   | 320 | 3/160    | $9.2 \cdot 10^{-4}$ |

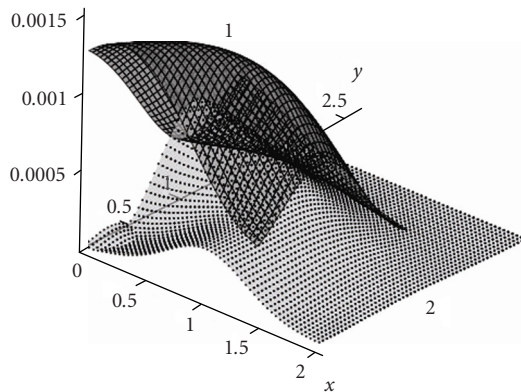


Figure 7.1. Spatial distribution of  $\varepsilon_1$ , (1)  $L = 3$ ; (2)  $L = 6$ .

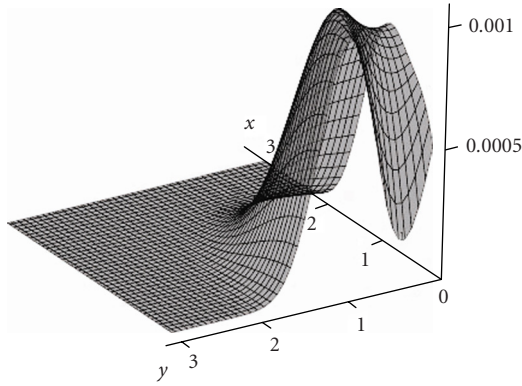


Figure 7.2. Spatial distribution of  $\varepsilon_2$  for  $N = 320$ .

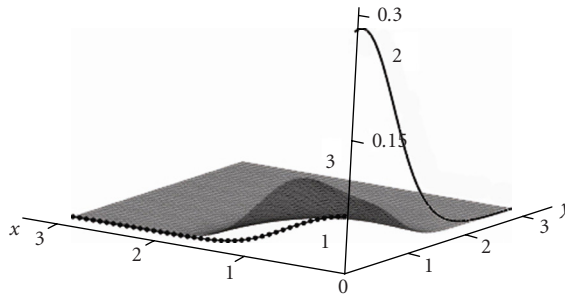


Figure 7.3. Numerically generated: (1)  $p_B(x)/1.5$ , (2)  $p_C(x)$ , (3)  $p_D(x, y)$ ,  $\lambda_s = 0.3$   $\lambda = 1.0$ . Note that  $p_B$  is divided by 1.5 due to scaling.

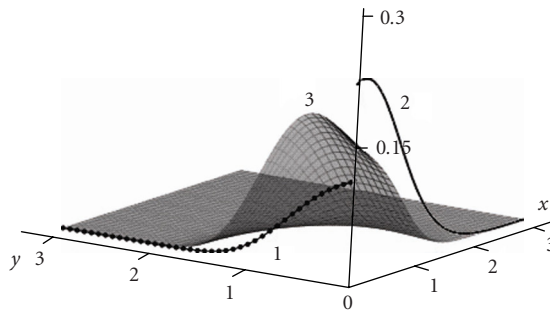


Figure 7.4. Numerically generated: (1)  $p_B(x)/1.5$ , (2)  $p_C(x)$ , (3)  $p_D(x, y)$ ,  $\lambda_s = 0.7$   $\lambda = 1.0$ . Note that  $p_B$  is divided by 1.5 due to scaling.

Figure 7.3 displays  $p_B(\cdot)$ ,  $p_C(\cdot)$ , and  $p_D(\cdot, \cdot)$  for  $\lambda = 1$ ,  $\lambda_s = 0.3$  and Figure 7.4 for  $\lambda = 1$ ,  $\lambda_s = 0.5$ . Figure 7.5 shows  $p_D(x, y)$  for various  $\lambda_s$ . Let  $\mathcal{A}_{\beta_1, \beta_2}(\lambda, \lambda_s)$  denote the long-run availability as a function of  $\lambda$  and  $\lambda_s$ .

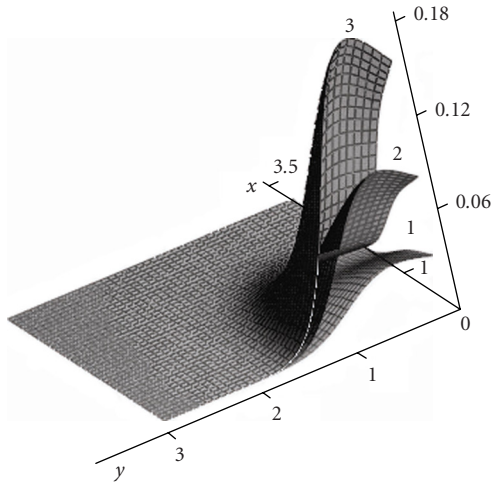


Figure 7.5. Numerically generated  $p_D(x, y)$ ,  $\lambda = 1.0$ , (1)  $\lambda_s = 0.1$ , (2)  $\lambda_s = 0.3$ , (3)  $\lambda_s = 0.7$ .

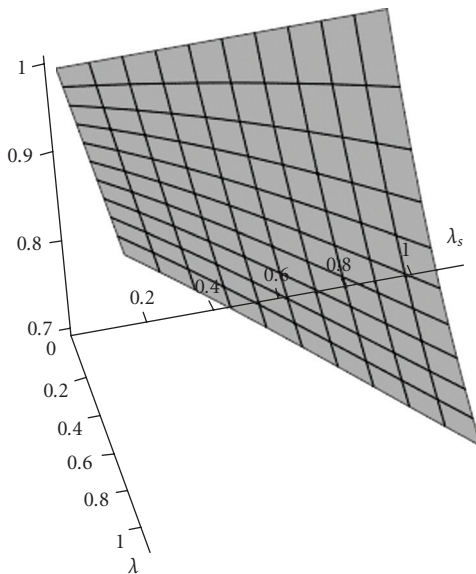


Figure 7.6. Numerically generated long-run availability.

Figure 7.6 shows that the long-run availability exhibits a nonlinear behavior for sufficiently large  $\lambda$  and  $\lambda_s$  (see also Table 7.3). Finally, Figure 7.7 displays the deviations  $d_1 := |\mathcal{A}_{2,2} - \mathcal{A}_{2,4}|$ ,  $d_2 := |\mathcal{A}_{2,2} - \mathcal{A}_{4,2}|$ ,  $d_3 := |\mathcal{A}_{2,2} - \mathcal{A}_{4,4}|$ . The plot reveals that  $\mathcal{A}$  is fairly insensitive for  $\beta$ -variations.

Table 7.3. Long-run availability  $\mathcal{A}_{2,2}(\lambda, \lambda_s)$ .

| $\lambda/\lambda_s$ | 0.1    | 0.2    | 0.3    | 0.4    | 0.5    | 0.6    | 0.7    | 0.8    | 0.9    | 1.0    |
|---------------------|--------|--------|--------|--------|--------|--------|--------|--------|--------|--------|
| 0.1                 | 0.9950 | 0.9895 | 0.9837 | 0.9775 | 0.9709 | 0.9640 | 0.9566 | 0.9489 | 0.9408 | 0.9324 |
| 0.2                 | 0.9908 | 0.9811 | 0.9706 | 0.9596 | 0.9480 | 0.9358 | 0.9231 | 0.9098 | 0.8962 | 0.8821 |
| 0.3                 | 0.9874 | 0.9740 | 0.9599 | 0.9450 | 0.9295 | 0.9133 | 0.8965 | 0.8792 | 0.8615 | 0.8434 |
| 0.4                 | 0.9845 | 0.9681 | 0.9509 | 0.9330 | 0.9143 | 0.8949 | 0.8750 | 0.8546 | 0.8338 | 0.8128 |
| 0.5                 | 0.9820 | 0.9631 | 0.9434 | 0.9229 | 0.9016 | 0.8797 | 0.8573 | 0.8345 | 0.8114 | 0.7882 |
| 0.6                 | 0.9798 | 0.9588 | 0.9369 | 0.9143 | 0.8909 | 0.8670 | 0.8426 | 0.8179 | 0.7930 | 0.7680 |
| 0.7                 | 0.9779 | 0.9550 | 0.9313 | 0.9069 | 0.8818 | 0.8562 | 0.8301 | 0.8039 | 0.7775 | 0.7512 |
| 0.8                 | 0.9762 | 0.9517 | 0.9265 | 0.9005 | 0.8740 | 0.8469 | 0.8195 | 0.7920 | 0.7644 | 0.7370 |
| 0.9                 | 0.9748 | 0.9488 | 0.9222 | 0.8949 | 0.8671 | 0.8389 | 0.8103 | 0.7817 | 0.7532 | 0.7249 |
| 1.0                 | 0.9734 | 0.9462 | 0.9184 | 0.8900 | 0.8611 | 0.8318 | 0.8024 | 0.7729 | 0.7435 | 0.7145 |

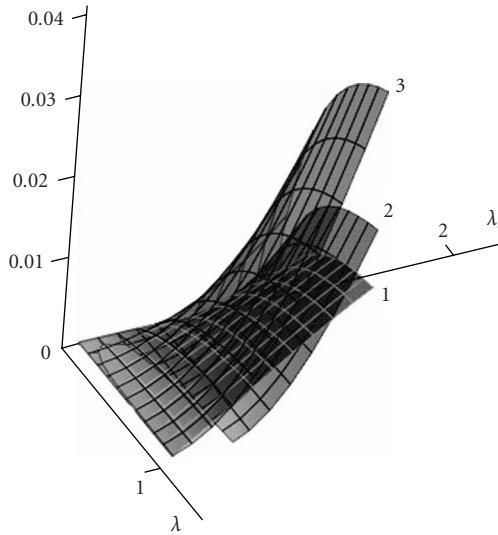


Figure 7.7. Spatial deviations  $d_i, i = 1, 2, 3$ .

### 8. Conclusion

An effective statistical analysis of the T-system requires the solution of coupled Hokstad-type differential equations. Our numerical solution procedure, endowed with a simple and robust algorithm, allows to compute and to analyze the long-run availability for a general class of current repair time distributions with tangible engineering applications.

### References

[1] J. R. Arora, *Reliability of a two-unit priority standby redundant system with finite repair capability*, IEEE Trans. Reliab. **R-25** (1976), 205–207.

- [2] ———, *Reliability of several standby priority redundant systems*, IEEE Trans. Reliab. **R-30** (1981), 123–132.
- [3] A. Birolini, *Quality and Reliability of Technical Systems*, Springer-Verlag, Berlin, 1994.
- [4] J. A. Buzacott, *Availability of priority redundant systems*, IEEE Trans. Reliab. **R-20** (1971), 60–63.
- [5] B. B. Fawzi and A. G. Hawkes, *Availability of a series system with replacement and repair*, J. Appl. Probab. **27** (1990), no. 4, 873–887.
- [6] I. B. Gertsbakh, *Statistical Reliability Theory, Probability: Pure and Applied*, vol. 4, Marcel Dekker, New York, 1989.
- [7] B. Gnedenko and I. A. Ushakov, *Probabilistic Reliability Engineering*, John Wiley & Sons, New York, 1995.
- [8] L. R. Goel and S. K. Singh, *Cost analysis of a two-unit priority standby system with imperfect switch, intermittent repair and arbitrary distributions*, IEEE Trans. Reliab. **R-35** (1986), 585–586.
- [9] R. Gupta and L. R. Goel, *Profit analysis of a two-unit priority standby system with administrative delay in repair*, Internat. J. Systems Sci. **20** (1998), 1703–1712.
- [10] W. Li and D. H. Shi, *Reliability analysis of a two-dissimilar-unit parallel redundant system with preemptive priority rule*, Microelectron. Reliab. **33** (1993), no. 10, 1447–1453.
- [11] H. Mine, *Repair priority effect on the availability of a two-unit system*, IEEE Trans. Reliab. **R-28** (1979), 325–326.
- [12] T. Nakagawa and S. Osaki, *Stochastic behaviour of a two-unit priority standby redundant system with repair*, Microelectron. Reliab. **14** (1975), no. 3, 309–313.
- [13] S. Osaki, *Reliability analysis of a two-unit standby redundant system with priority*, Can. Oper. Res. Soc. J. **8** (1970), 60–62.
- [14] H. Pham, *Recent Advances in Reliability and Quality Engineering*, World Scientific Publishing, Singapore, 2001.
- [15] M. Shaked and J. G. Shanthikumar, *Reliability and maintainability*, Stochastic Models (D. P. Heyman and M. J. Sobel, eds.), Handbooks Oper. Res. Management Sci., vol. 2, North-Holland, Amsterdam, 1990, pp. 653–713.
- [16] D.-H. Shi and L. Liu, *Availability analysis of a two-unit series system with a priority shut-off rule*, Naval Res. Logist. **43** (1996), no. 7, 1009–1024.
- [17] R. Subramanian and N. Ravichandran, *Probabilistic analysis of a two-unit standby redundant system with finite repair capacity*, Opsearch **17** (1980), no. 2-3, 71–80.
- [18] ———, *Analysis of a two unit warm standby system*, Opsearch **21** (1984), 23–29.
- [19] K. Val'des Kastro, *Optimal policies in a priority standby model*, Vestnik Moskov. Univ. Ser. I Mat. Mekh. **41** (1986), no. 4, 10–15.
- [20] E. J. Vanderperre, *Reliability analysis of a two-unit cold standby redundant system subject to a priority rule*, Cahiers Centre Études Rech. Opér. **31** (1989), no. 1-2, 159–166.
- [21] ———, *Long-run availability of a two-unit standby system subjected to a priority rule*, Bull. Belg. Math. Soc. Simon Stevin **7** (2000), no. 3, 355–364.
- [22] E. J. Vanderperre, S. S. Makhanov, and S. Suchatvejapoom, *Long-run availability of a repairable parallel system*, Microelectron. Reliab. **37** (1997), no. 3, 525–527.

Edmond J. Vanderperre: Department of Quantitative Management, University of South Africa,  
P.O. Box 392, Pretoria 0003, South Africa  
*E-mail address:* edmondvanderperre@hotmail.com

Stanislav S. Makhanov: Faculty of Information Technology, Sirindhorn International Institute of  
Technology, Thammasat University, P.O. Box 22, Patumthani 12121, Thailand  
*E-mail address:* makhanov@siit.tu.ac.th